*J. Physiol.* (1979), **293**, *pp.* 197–215
*With 9 text-figures*
*Printed in Great Britain*



# CHANGES IN MOTONEURONE ELECTRICAL PROPERTIES FOLLOWING AXOTOMY

BY BENGT GUSTAFSSON
*From the Department of Physiology, University of Göteborg, Göteborg, Sweden*

(*Received 22 January 1979*)

SUMMARY

1. Passive electrical properties, afterpotential properties and the pattern of repetitive discharge induced by constant current injection were studied in axotomized lumbar motoneurones.

2. Following axotomy, the motoneurones showed a larger input resistance and membrane time constant, but had a normal electrotonic length.

3. Duration and peak amplitude of the afterhyperpolarization (ahp) were on average unchanged following axotomy. There was, however, a significant reduction in the conductance underlying the ahp. The distribution of values for ahp duration was also narrower following axotomy, with an absence of long and short values.

4. As in normal motoneurones, the ahp conductance, calculated from the voltage, decayed in an approximately exponential manner with a phase of slower decay corresponding to the hyperpolarizing phase of the ahp. The phase of slower decay was, however, less accentuated and several axotomized motoneurones showed an exponential decay of the ahp conductance.

5. The frequency–current (*f–I*) curves for the first interspike intervals were, as in normal motoneurones, non-linear, deviating upwards at higher frequencies. The steady-state *f–I* relations were, however, linear in most of the axotomized neurones. The slopes of the *f–I* curves were steeper following axotomy. These steeper slopes were well correlated with the decreased ahp conductance.

6. The interspike voltage trajectories were similar to those in normal motoneurones, i.e. concave at low current strength and changing to a convex shape with increasing current injection. The changes in the trajectory shape were not correlated with the changes in the slope of the *f–I* curves.

7. It is concluded that the afterhyperpolarization conductance is the major factor in the regulation of repetitive firing in axotomized motoneurones.

## INTRODUCTION

At present there is good evidence that the afterhyperpolarization is the main factor in the control of repetitive firing in lumbar motoneurones (Kernell & Sjöholm, 1973; Baldissera & Gustafsson, 1974*b*, *c*; Baldissera, Gustafsson & Parmiggiani, 1978). However, the participation of other factors, e.g. changes in the amount of invasion of the spike into the dendritic tree, has been discussed (Granit, Kernell & Lamarre, 1966; Schwindt & Calvin, 1972). Recently, Heyer & Llinás (1977) proposed

0022-3751/79/4470-0975 $01.50 

that the upward deviation of the frequency–current ($f$–$I$) relation, i.e. the entry into the 'secondary range' (Kernell, 1965) in normal motoneurones is related to the initiation of dendritic spikes. This proposal was based on the observation that the firing pattern in axotomized motoneurones, in which the dendritic excitability is high (e.g. Eccles, Libet & Young, 1958; Kuno & Llinás, 1970), was similar to that in normal motoneurones after the upward deviation of the $f$–$I$ curve. Accordingly, firing in neurones which normally have a high dendritic excitability may not be primarily controlled by the ahp.

Following axotomy, there are also changes in the ahp (Kuno, Miyata & Muñoz-Martinez, 1974; Heyer & Llinás, 1977). The aim of the present study was thus to determine to which extent changes in the characteristics of the ahp are responsible for modifications in the firing pattern following axotomy.

## METHODS

The experimental results presented were obtained from nine cats. In five cats ventral roots L7 and S1 were sectioned intradurally on the left side, 2–3 weeks before the experiments. In two cats the nerves to the left medial gastrocnemius and soleus muscles were cut close to the muscles, 4 and 8 weeks before the experiments. Two cats not operated before the experiment were used as controls.

Cats were anaesthetized with pentobarbitone (Nembutal, Abbott) 35–40 mg/kg intraperitoneally, supplemented with small doses (5 mg/kg) when needed, immobilized with gallamine triethiodide (Flaxedil, May & Baker Ltd) and artificially respired. Bilateral pneumothorax was always performed to reduce respiratory movements. End-tidal $CO_2$ was monitored on a Beckman medical gas analyser and kept within 4·5–5·5 %. Arterial blood pressure was monitored continuously and was always above 80 mmHg. Rectal temperature was kept within 37–39 °C.

Intracellular recordings from $\alpha$-motoneurones were obtained in L7–S1 segments using single-barelled micro-electrodes filled with 2 M-K citrate. The microelectrodes had broken tips with diameters 1·5–2 $\mu$m and a resistance when measured in saline of 2–5 MΩ. Motoneurones were identified by antidromic invasion from the cut ventral roots or from the cut peripheral nerves.

Afterhyperpolarizations (ahps) were studied following spikes evoked by short (< 1 msec) current pulses. The ahp duration was measured from the spike onset to where the ahp crossed the base line. The input resistance was measured from the voltage drop produced by injecting small (2–5 nA), short (15–25 msec) current pulses through the recording micro-electrode. The device used allowed compensation of the voltage drop across the micro-electrode resistance (Eide, 1968). The membrane time constant ($\tau_m$) was estimated by plotting the voltage transient ($v$) as ln ($v$) against time. The first equalizing time constant ($\tau_1$) was similarly estimated after peeling off the first exponential term. Voltage and duration values for the plotting procedure were obtained on a Hewlett–Packard digitizer (9864A). The electrotonic length ($L$) was calculated from the expression

$$L = \frac{\pi}{\sqrt{\tau_m/\tau_1 - 1}} \text{ (Rall, 1969).}$$

The computations in section III were done as described in a previous paper (Baldissera & Gustafsson, 1974*a*).

The repetitive firing was induced by injection of 200 msec long, depolarizing current pulses at a frequency of 0·2/sec. The current strength was changed stepwise from low to high values and back again and three current pulses were applied in succession at each intensity level. A stable sequence of measurements was then selected for the construction of the $f$–$I$ curves.

Only motoneurones showing stable spike amplitudes of more than 75 mV were used in the present study. The spike amplitudes were on the average 81 mV in the normal population (ranging from 75 to 92 mV, $n$ = 56) and 86 mV (ranging from 75 to 109 mV, $n$ = 68) in the axotomized population.

## RESULTS

### *I. Afterpotentials*

In normal motoneurones the soma-dendritic spike is followed by an afterhyperpolarization (ahp), which reaches a peak amplitude of approximately 5 mV 10–20 msec after spike onset and lasts 40–200 msec. The rapid falling phase of the spike is usually not immediately followed by the ahp, but by a phase of slow repolarization, the delayed depolarization (Fig. 1*A*). Previous studies have shown that the ahp

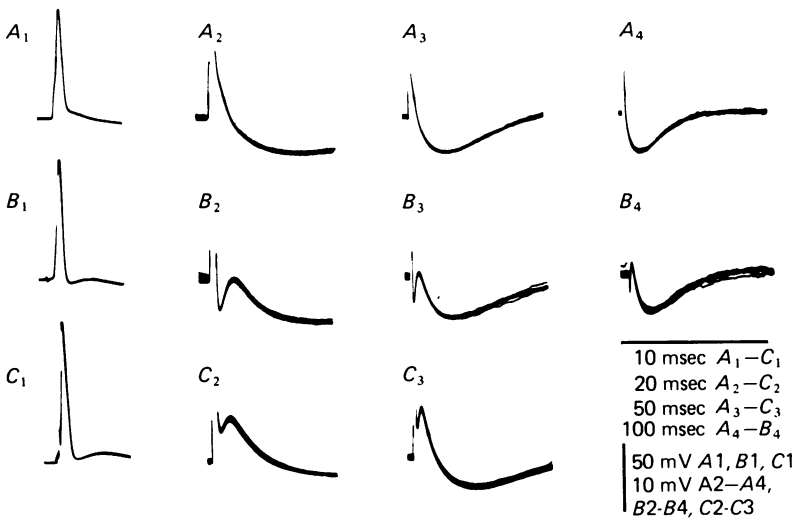


Fig. 1. Spike potentials and afterpotentials in normal and axotomized motoneurones. *A*, normal motoneurone. *B*, *C*, two different axotomized motoneurones. The spikes in *A* and *B* are evoked by stimulation of the ventral root. The spike in *C* is evoked by a short intracellular current pulse. Observe the more prominent delayed depolarizations in the axotomized neurones in *B* and *C* and the hyperpolarizing undershoot in *B*. Note also the brief IS-SD delay in the axotomized neurones. For further details, see text.

duration can change following axotomy, decreasing in motoneurones to the slow soleus (Sol) muscle while increasing in motoneurones to the medial gastrocnemius (mg) muscle (Kuno *et al.* 1974). A decrease in ahp peak amplitude was also noted by Heyer & Llinás (1977). In the present experiments peak amplitude, time to peak amplitude (from spike onset) and duration of ahps following spikes evoked at resting level were measured in normal and axotomized motoneurones. The distribution of the values of these parameters is shown in the histograms in Fig. 2 and the mean values are given in Table 1. The axotomized neurones consist of two groups, one studied 2–3 weeks following ventral root section and another (with mg-Sol motoneurones) studied 5–8 weeks following section of the peripheral nerve. There were few differences between the two groups with respect to changes in ahp and firing properties. However, in order to compare with other results, the values from these groups are shown separately. For the normal motoneurones the values are also given for a subgroup consisting of triceps surae motoneurones. It can be seen from Table 1 that there are no large differences in the mean values of the studied

TABLE 1. Mean values of parameters studied in both normal and axotomized motoneurones

| | Ahp peak amplitude (mV) | Time to peak ahp (msec) | Ahp duration (msec) |
|---|---|---|---|
| Axotomized motoneurones | | | |
| Ventral root cut | $4{\cdot}5 \pm 1{\cdot}1$ $n = 47$ | $16{\cdot}0 \pm 3{\cdot}2$ $n = 47$ | $88 \pm 16$ $n = 42$ |
| Nerve cut | $3{\cdot}7 \pm 0{\cdot}9$ $n = 21$ | $18{\cdot}1 \pm 2{\cdot}6$ $n = 20$ | $94 \pm 19$ $n = 18$ |
| Normal motoneurones | | | |
| Total | $4{\cdot}5 \pm 1{\cdot}5$ $n = 56$ | $15{\cdot}4 \pm 3{\cdot}8$ $n = 53$ | $79 \pm 27$ $n = 53$ |
| Triceps surae | $4{\cdot}6 \pm 1{\cdot}7$ $n = 15$ | $16{\cdot}5 \pm 5{\cdot}1$ $n = 15$ | $89 \pm 41$ $n = 15$ |

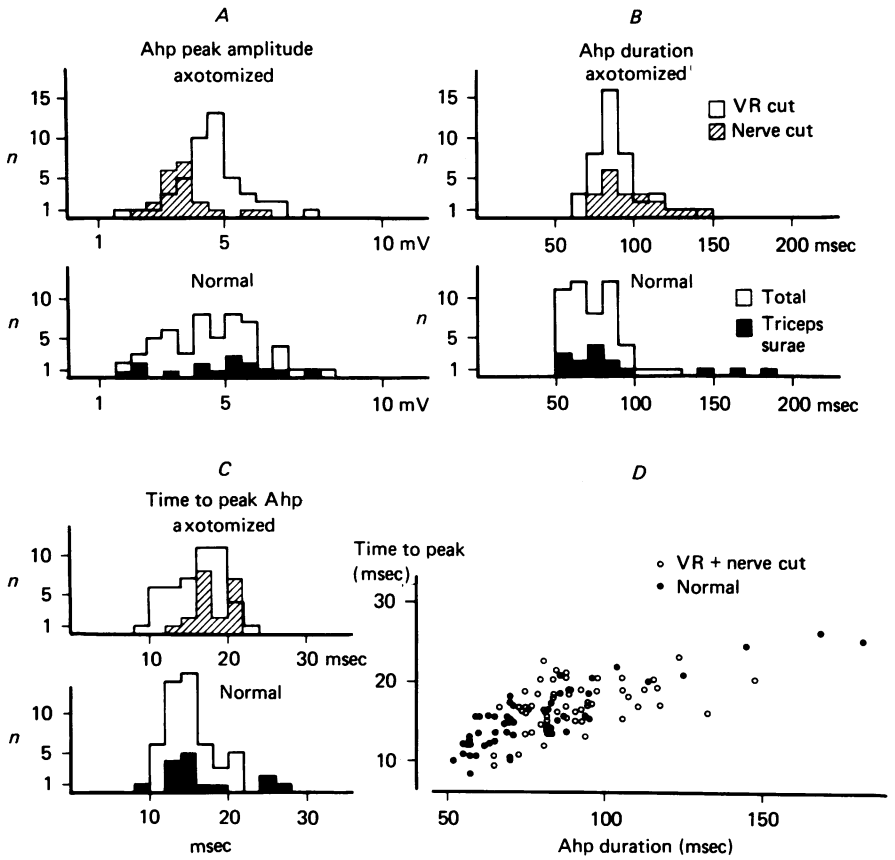


Fig. 2. Ahp parameters in normal and axotomized motoneurones. *A*, *B* and *C*, distributions of ahp peak amplitude (*A*), ahp duration (*B*) and time to peak ahp (*C*) in axotomized (upper histograms) and normal (lower histograms) motoneurones. Distributions following ventral root section and nerve section are shown separately as indicated in *B*. For the normal population the distributions are given for all the motoneurones and for a subgroup of triceps surae motoneurones as indicated in *B*. The number of motoneurones in each group is given in Table 1. *D*, relation between ahp duration and time to peak ahp for normal motoneurones (filled circles) and axotomized neurones (open circles). For further details, see text.

parameters between normal and axotomized neurones. There is only for the axotomized mg-Sol population some decrease in ahp peak amplitude and a slight increase in ahp duration following ventral root section. These changes were not statistically significant ($P > 0{\cdot}05$). Thus, with respect to amplitude and time course the ahp is on the average rather unaffected by axotomy.

There are, however, some changes in the distribution of the ahp values following axotomy as can be seen from the histograms in Fig. 2. The distributions are narrower for the ahp peak amplitude and duration. For instance, there are very few values of ahp duration less than 70 msec in the axotomized population when compared to the normal one. Axotomized soleus motoneurones showed also shorter than normal ahp durations (cf. Kuno *et al.* 1974). It could also be noted that the values for the time to peak ahp are differently skewed in the two populations, the peak distribution shifted from 12 to 16 msec for the normal motoneurones to 16–20 msec for the axotomized ones. As shown for normal motoneurones in Fig. 2*D* there is a positive correlation between ahp duration and the time to peak ahp. It can be seen from this plot that with ahp durations between 70 and 100 msec (as in axotomized neurones) the time to peak ahp should vary from 14 to 20 msec. Similarly, lack of long time to peaks could be related to the disappearance of ahps with long duration.

Following axotomy, there were not only changes in the ahp but also in the delayed depolarization. As illustrated from two axotomized neurones in Fig. 1*B*, *C* this depolarization could assume the shape of a prominent depolarizing hump, interrupting the falling phase of the spike. Such depolarizing humps were found in 42/68 axotomized neurones following spikes with amplitudes in excess of 75 mV and evoked at resting level, compared to 2/56 in normal motoneurones. The fraction of cells with a depolarizing hump was substantially larger in the population with ventral roots cut (35/47) than with the nerves cut (7/21). In the axotomized neurone in Fig. 1*B* the falling phase of the spike ends in a hyperpolarizing undershoot. Similar undershoots with spikes evoked at resting level were observed in 19/68 axotomized neurones and in none of the normal ones.

*II. Passive electrical properties*

Eccles *et al.* (1958) and Kuno & Llinás (1970) found no significant changes in input resistance ($R_{in}$) following ventral root section. Kuno *et al.* (1974), however, described a clear increase in $R_{in}$ in axotomized mg motoneurones. In the present study input resistance, membrane time constant and electrotonic length were calculated (see Methods) for normal and axotomized neurones. The distribution of such values is shown in the histograms in Fig. 3 and the mean values are given in Table 2. It can be observed from Table 2 that there is a significant increase in $R_{in}$ ($P < 0{\cdot}01$ when comparing ventral root cut with the total normal material and $P < 0{\cdot}05$ for the triceps surae), a small (but significant, $P < 0{\cdot}02$) increase in time constant following ventral root section and no obvious change in electrotonic length following axotomy. There is also, as shown in the histogram in Fig. 3*A*, a notable change in the distribution of $R_{in}$ values. In the normal population there is a tendency for a bimodal distribution with values above and below 1·5 MΩ. On the other hand, in the axotomized population there is a unimodal distribution with no values below 1·4 MΩ. In triceps surae motoneurones, Burke & Bruggencate (1971) noted no correlation

TABLE 2. Comparison of passive electrical properties studied in normal and axotomized motoneurones

| | Input resistance (MΩ) | Time constant (msec) | Electrotonic length (L) |
|---|---|---|---|
| Axotomized motoneurones | | | |
| Ventral root cut | $2{\cdot}18 \pm 0{\cdot}53$ $n = 53$ | $6{\cdot}44 \pm 1{\cdot}70$ $n = 36$ | $1{\cdot}17 \pm 0{\cdot}14$ $n = 23$ |
| Nerve cut | $2{\cdot}19 \pm 0{\cdot}40$ $n = 21$ | $5{\cdot}77 \pm 1{\cdot}20$ $n = 16$ | $1{\cdot}25 \pm 0{\cdot}15$ $n = 12$ |
| Normal motoneurones | | | |
| Total | $1{\cdot}32 \pm 0{\cdot}53$ $n = 52$ | $5{\cdot}03 \pm 1{\cdot}68$ $n = 45$ | $1{\cdot}24 \pm 0{\cdot}15$ $n = 39$ |
| Triceps surae | $1{\cdot}59 \pm 0{\cdot}66$ $n = 12$ | $5{\cdot}85 \pm 1{\cdot}92$ $n = 12$ | $1{\cdot}20 \pm 0{\cdot}17$ $n = 11$ |

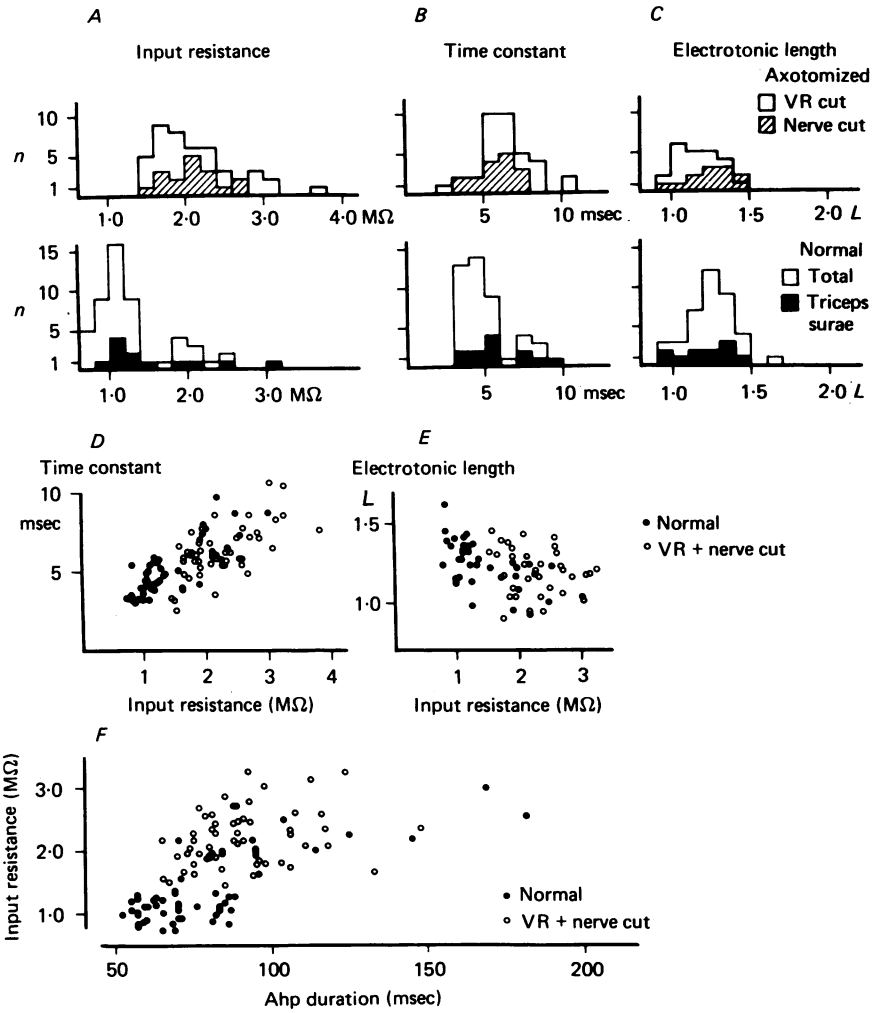


Fig. 3. Passive electrical properties of normal and axotomized motoneurones. *A*, *B* and *C*, distributions of input resistance (*A*), time constant (*B*) and electrotonic length (*C*) in axotomized (upper histograms) and normal (lower histograms) motoneurones. Symbols as in Fig. 2. The number of motoneurones in each group is given in Table 2. *D*, *E* and *F*, relations between input resistance and membrane time constant (*D*), input resistance and electrotonic length (*E*) and ahp duration and input resistance (*F*) for normal (filled circles) and axotomized (open circles) motoneurones. For further details, see text.

between the time constant and $R_{in}$ or between the electrotonic length and $R_{in}$. In the present normal material there was a tendency for both the time constant and the electrotonic length to change with $R_{in}$, the time constant increasing and the electrotonic length decreasing with increasing $R_{in}$ (Fig. 3*D*, *E*, filled circles). The axotomized neurones also show a correlation between time constant and $R_{in}$ (Fig. 3*D*, open circles). The change in time constant following axotomy seems well related to the larger $R_{in}$ in the axotomized cells. On the other hand, the increase in $R_{in}$ following axotomy does not seem to be connected with a reduction in the electrotonic length (Fig. 3*E*, open circles).

As already discussed by Kernell (1966) there is a relation between the ahp duration and the input resistance, the ahp being shorter in cells with low input resistance (Fig. 3*F*, filled circles). Following axotomy there is an increase in both $R_{in}$ and ahp duration. However, as shown in Fig. 3*F* (compare filled and open circles) the increase in input resistance seems out of proportion to the change in ahp duration. Selecting cells with ahp durations between 70 and 100 msec (mean duration 82 msec, $n = 24$, normal motoneurones; 84 msec, $n = 44$, axotomized motoneurones), the corresponding mean $R_{in}$ values are 1·3 MΩ ± 0·09 S.E. and 2·17 MΩ ± 0·06 S.E.; i.e. a clear significant difference.

*III. Ahp conductance*

It was shown in section I that the ahp peak amplitude was virtually unchanged following axotomy. On the other hand, as shown in section II, there was a substantial increase in $R_{in}$ following axotomy. These two results must mean that the current underlying the ahp must be less in the axotomized neurones than in the normal ones. To measure the current underlying the ahp, the peak amplitude was divided by the input resistance. As expected there was a considerable difference, the average ahp current decreased from 3·7 nA (fifty-five normal motoneurones) to 2·1 nA (forty-six motoneurones with ventral root cut) and 1·7 nA (twenty-one motoneurones with nerve cut). The distribution of values was also similar to the ahp peak amplitude distribution, narrower for the axotomized population (Fig. 4*E*). This decrease in ahp current could be due to a reduction either in the ahp conductance or in the driving force. The first alternative was tested by measuring the conductance change at the peak of the ahp with the current pulse technique (see Methods). Assuming a constant driving force, the ahp peak amplitude should be only related to the conductance change during the ahp. The relation between ahp conductance change and ahp peak amplitude should thus be the same for normal and axotomized motoneurones. The relation between ahp peak amplitude and conductance change is shown in Fig. 4*G* for twenty-eight motoneurones, seventeen normal (filled circles) and eleven axotomized (open circles). This graph shows first a good correlation between ahp conductance change and peak amplitude suggesting that the main factor deciding the variability in peak amplitude is the magnitude of conductance change rather than differences in driving force. Moreover, the values from normal and axotomized neurones overlap well, suggesting the same magnitude of driving force for the two populations. On average, the ahp peak amplitudes and conductance changes were 4·6 mV, 43 % for the normal and 5·2 mV, 51 % for the axotomized neurones. This similarity in conductance change should be compared with the reduction in ahp current from average values of 3·8–2·3 nA for the same cells.

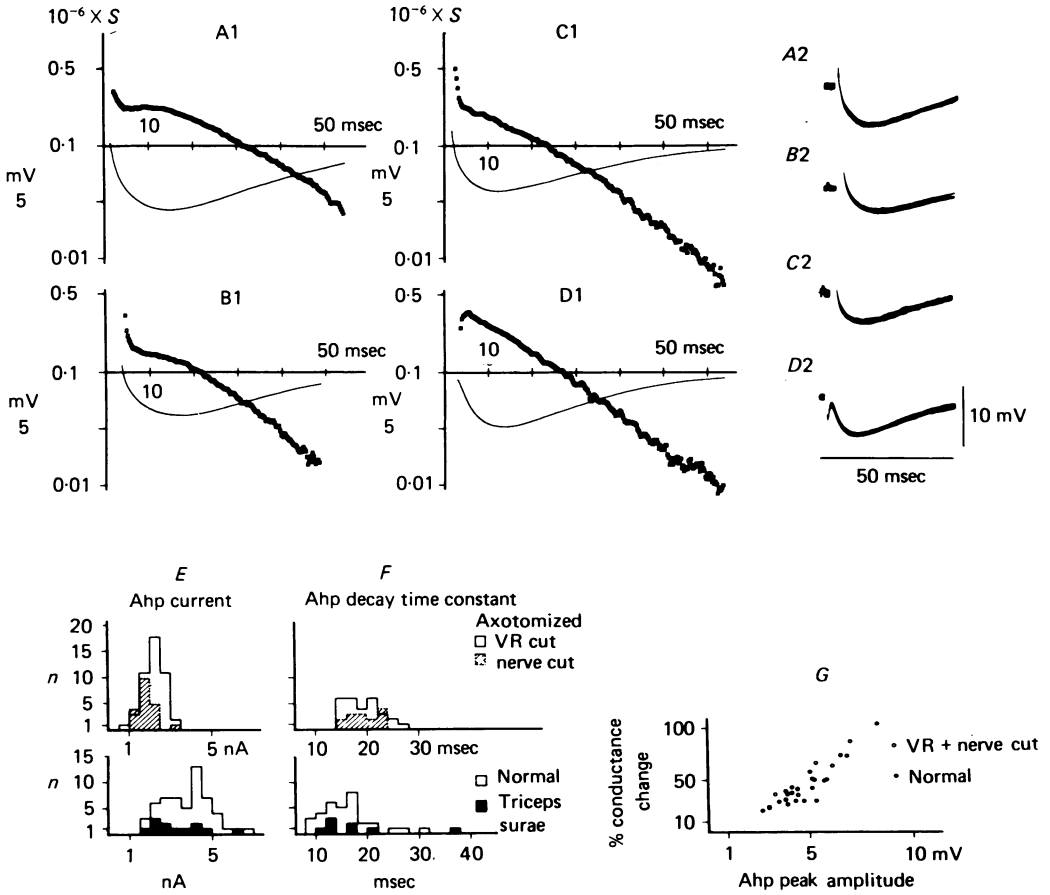


Fig. 4. Ahp conductance in axotomized motoneurones. $A_1$–$D_1$, calculated time course of the conductance change underlying the ahp. Cell input resistances and capacitances were 2·5 MΩ, 2·3 nF (*A*), 2·5 MΩ, 3·0 nF (*B*), 2·0 MΩ, 3·3 nF (*C*) and 1·9 MΩ, 4·0 nF (*D*). $A_2$–$D_2$, records of the ahps for the cells in $A_1$–$D_1$. *E* and *F*, distributions of ahp current (as defined in the text) (*E*) and ahp decay time constant (*F*) in axotomized (upper histograms) and normal (lower histograms) motoneurones. Distributions following ventral root section and nerve section are shown separately as indicated in *F*. For the normal population the distributions are given for all motoneurones and for the subgroup of triceps surae motoneurones as indicated in *F*. The average values for the decay time constant were for axotomized neurones 19·2 msec (after ventral root (*VR*) section, $n = 28$), 19·2 msec (after nerve section, $n = 13$), 16·2 msec (normal motoneurones, $n = 34$). *G*, relation between ahp peak amplitude and the percentage conductance change during the ahp as measured with current pulses. Normal motoneurones (filled circles), axotomized neurones (open circles). For further details see text.

The conductance during the ahp decays in an approximately exponential manner in normal motoneurones. This exponential decay is generally preceded by a phase of slower decay or even a plateau corresponding to the slower hyperpolarizing phase of the ahp (Baldissera & Gustafsson, 1974*a*). To investigate the possibility of changes in the time course following axotomy, the conductance time course was evaluated by

calculating it from the ahp voltage, as previously described (Baldissera & Gustafsson, 1974*a*). Evaluated in that way conductance time courses generally showed similar characteristics in axotomized and normal motoneurones, i.e. an exponential decay preceded by a phase of slower decay or of a plateau (Fig. 4*A–D*). Following axotomy there was thus no qualitative change in the time course. There was, however, a tendency for the time course to be closer to exponential. Of the forty-seven axotomized neurones studied a large fraction (17/47) was judged to have time courses similar to those in Fig. 4*C*, *D*, i.e. with small deviations from exponentiality even during the hyperpolarizing phase of the ahp (definitely more exponential than that in 4*B*) and in six of these neurones the time course was very close to exponential (Fig. 4*D*). For the normal population of forty neurones only five showed time courses as in Fig. 4*C* and an exponential decay (4*D*) was only observed in one cell.

As shown in section I the distribution of the values for ahp duration was narrower following axotomy. As shown in Fig. 4*F* there was a similar shift in the distribution of values for the time constant of the exponential decay of the conductance following axotomy.

In summary, there is following axotomy an increase in the input resistance, a decrease in ahp current and a small lengthening of the ahp duration. These changes were found for the motoneurone population as a whole following ventral root section and for triceps surae motoneurones following nerve section (no average change in ahp duration). The same differences also exist for identified motoneurones following ventral root section, e.g. for hamstring motoneurones. Here input resistance, ahp current and ahp duration change from 1·0 MΩ, 4·1 nA and 68 msec ($n$ = 22) to 2·2 MΩ, 2·3 nA and 85 msec ($n$ = 12).

*IV. Firing behaviour*

Heyer & Llinás (1977) reported that following axotomy the frequency–current ($f$–$I$) relations were over most of the frequency range linear for all intervals. No upward deviation of the $f$–$I$ curves was described at higher current intensities, as is the case in normal motoneurones.

Typical $f$–$I$ relations from an axotomized neurone are shown in Fig. 5*A*. It can be seen that the $f$–$I$ relations for the first intervals after current onset are non-linear, deviating upwards with increasing current intensities. For the steady state the $f$–$I$ relation is approximately linear over the whole range as in many normal motoneurones. Upward deviations of the first interval curve were observed in all but one of the present twenty-six axotomized neurones (nineteen with ventral root cut and seven with nerve cut). The intersection between two lines approximating the shape of the first interval $f$–$I$ curve occurred at frequencies between 40 and 90 impulses/sec (mean value 62 impulses/sec). This is comparable to transition frequencies in normal motoneurones (40–110 impulses/sec, mean 66, $n$ = 13) (see also Kernell, 1965). In the only axotomized neurone without an upward deviation the linear range extended up to 110 impulses/sec before deviating downward from linearity.

For the neurone illustrated in Fig. 5 the transition frequency for the upward deviation is higher for the second and third intervals than for the first interval. The steady state curve extends linearly up to 100 impulses/sec, i.e. considerably higher than the transition frequency for the first interval. This extension of the linear region

to higher frequencies with later intervals was usually found in axotomized neurones. However, in the majority upward deviations were still observed for the second and third intervals (21/26). The transition for the second and third intervals occurred at somewhat higher frequencies than for the first interval (45–100 impulses/sec, mean value 75). In the steady state, upward deviations of the *f–I* curve were found only in two cells. These upward deviations occurred at 70 and 80 impulses/sec respectively, somewhat higher than the transition frequencies for the first interval (50

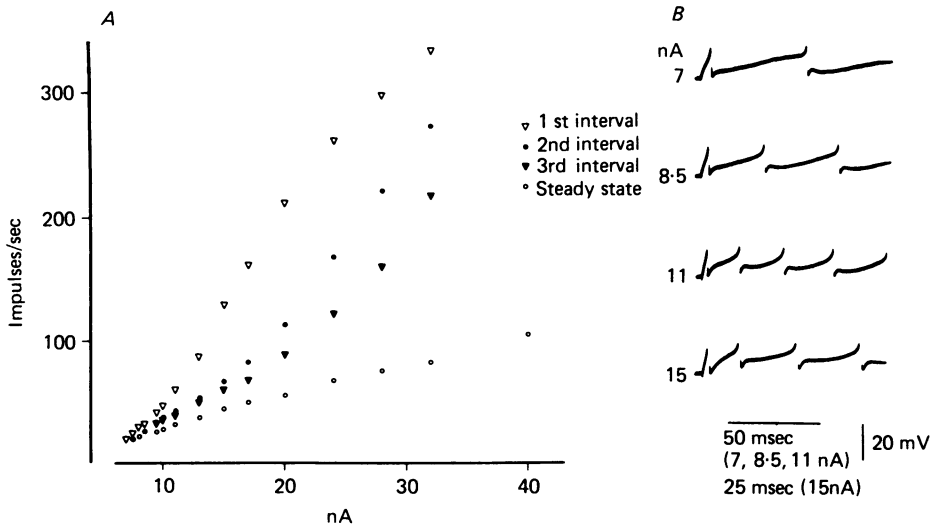


Fig. 5. Frequency–current relations in an axotomized motoneurone (after ventral root section). *A*, reciprocals of the first intervals (open triangles), second intervals (filled circles) and third intervals (filled triangles) after the current onset, together with the frequency at 0·2 sec (open circles) are plotted against the amount of injected current. Each point in the graph represents the average of three trials. The 0·2 sec values are the mean of two to three successive intervals. *B*, sample records of the interspike voltage trajectories for the first few intervals after current onset.

and 55 impulses/sec). The change in *f–I* slope was in both cases quite small, the slope ratio being only 1·4 and 1·25. Thus, 24/26 cells showed a single linear relation in steady state. This is considerably more than in the control material where 8/13 had a single linear relation in the steady state (50 %, Kernell, 1965). At the highest current intensities fifteen of the axotomized neurones gave only a transient or irregular discharge. They were thus incapable of reaching higher discharge frequencies. It is possible that an upward deviation could have occurred for the remaining neurones if higher current intensities had been used. This was also true for 4/5 cells not showing upward deviations for the second and third intervals.

The slope of the steeper segment of the first interval curve was quite variable, ranging from 7 to 95 impulses $sec^{-1}\,nA^{-1}$, and centred around 15–35 impulses $sec^{-1}\,nA^{-1}$. In five cells (ventral root cut) the approximated slope was very steep, 50–95 impulses $sec^{-1}\,nA^{-1}$. In these cells the delayed depolarization was very pronounced and it clearly facilitated the firing at higher frequencies (Fig. 7*C*). Short

intervals, caused by the delayed depolarization (crossing the threshold level), appeared also in these cells during the repetitive firing. For the remaining twelve neurones (ventral root cut) (as well as for the second and third intervals for all seventeen neurones) the upward deviation was continuous with slopes varying from 18 to 34 impulses $sec^{-1}$ $nA^{-1}$. The ratio between the two segments of the first interval curve varied from 2·0 to 6·2 with a mean value of 3·4 ($n$ = 12). For the axotomized mg-Sol motoneurones the slope of the steeper segment was less, ranging from 7 to 17

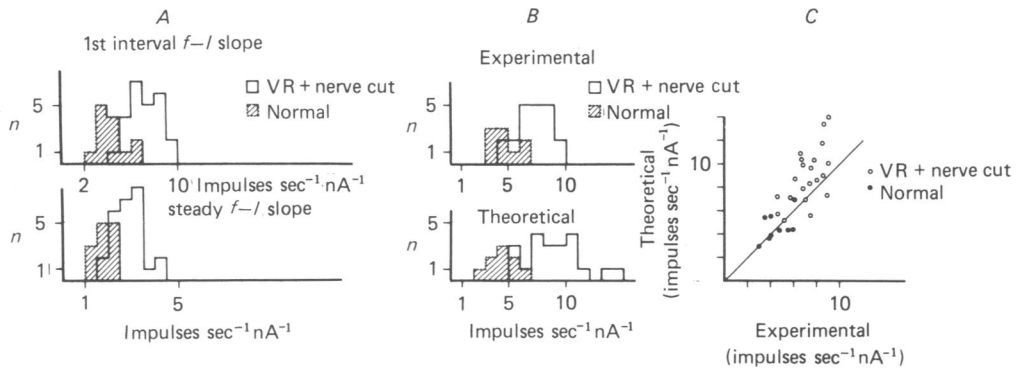


Fig. 6. Frequency–current slopes in normal and axotomized motoneurones. *A*, frequency–current slopes for the first interval (upper histograms) and for the steady *f–I* relation (lower histogram) for normal and axotomized motoneurones, symbols as indicated in the Figure. Note that the histograms for normal and axotomized motoneurones are overlapping. *B*, distributions of the first interval *f–I* relations in normal and axotomized motoneurones, as found experimentally (upper histograms) and as calculated from the ahp conductance (see text) in the same cells (lower histograms). *C*, the experimentally found first interval *f–I* relation is plotted on the abscissa against the calculated one for normal (filled circles) and axotomized (open circles) motoneurones. The drawn line indicates equivalence between the experimental and calculated values. For further details, see text.

impulses $sec^{-1}$ $nA^{-1}$, giving slope ratios of 1·2–3·7 (mean value 2·0, $n$ = 6). In the normal motoneurones the slope of the steeper segment varied between 13·5–40 impulses $sec^{-1}$ $nA^{-1}$ ($n$ = 11), excluding two cells with slopes of around 80 impulses $sec^{-1}$ $nA^{-1}$. The *f–I* slope ratio varied for these eleven cells between 2·8 and 9·8 with a mean value of 6·0, i.e. considerably larger than for the axotomized ones. The steep upward deviation in the two excluded cells was not related to a delayed depolarization but was rather given by a hump resulting from the plateau in the ahp conductance (cf. Baldissera & Gustafsson, 1974*b*).

Axotomized motoneurones showed, according to Heyer & Llinás (1977), not only *f–I* relations that were linear but these relations had also much steeper slopes than the lower linear part of the curves in normal motoneurones. In fact, the steady-state *f–I* slopes were, following axotomy, similar to those of the upper linear segment of the curves in normal motoneurones. Steeper slopes following axotomy were also observed in the present study (Fig. 6*A*). For example, for the steady-state *f–I* relation there was a significant increase in slope ($P$ < 0·01) from 1·8 impulses $sec^{-1}$ $nA^{-1}$ (normal motoneurones $n$ = 13) to 2·8 impulses $sec^{-1}$ $nA^{-1}$ (axotomized motoneurones

$n$ = 26). As can be observed in the histograms in Fig. 6*A* the shift in mean values was related to a general shift in the distribution of the *f–I* slope values. This shift in average slope is considerably less than that reported by Heyer & Llinás (1977) (1·9–7·2 impulses $sec^{-1}$ $nA^{-1}$). It can be noted that even the highest value encountered in the present experiments (4·1 impulses $sec^{-1}$ $nA^{-1}$ falls short of their mean value of 7·2 impulses $sec^{-1}$ $nA^{-1}$. However, this value (4·1 impulses $sec^{-1}$ $nA^{-1}$; cell in Fig. 5) is comparable to that in their illustrated neurone (4·2 impulses $sec^{-1}$ $nA^{-1}$; Fig. 2, Heyer & Llinás, 1977). The change of *f–I* slope from the first to the second interval was much the same in normal and axotomized neurones (*f–I* slope ratio 1·8 and 1·6 respectively). However, the further change in *f–I* slope from the second interval to the steady state was more pronounced following axotomy (*f–I* slope ratio 1·3 and 1·7, respectively).

The tendency for a short first interspike interval to be followed by long succeeding intervals was reduced following axotomy. In the normal motoneurones a first interspike interval of 5 msec was followed by a second interval with an instantaneous frequency of 59 impulses $sec^{-1}$ $nA^{-1}$ (range 31–78, $n$ = 13). Following axotomy the corresponding figures were 105 impulses $sec^{-1}$ $nA^{-1}$ (range 64–148, $n$ = 17) when excluding the five cells where the first interval was facilitated by the delayed depolarization. This exclusion seems reasonable since no such facilitation was present in the normal material.

In normal motoneurones the second interval can become longer than the third one when the first interval enters the steeper segment of the *f–I* curve (Baldissera & Gustafsson, 1974*c*). This behaviour was also observed in the five axotomized neurones where the first interval shortened due to the presence of a delayed depolarization. However, in the remaining twenty-one neurones no such crossing was observed. This behaviour was in contrast to that in normal motoneurones where a clear crossing was observed in six of the eleven neurones with a continuous upward deviation.

*V. Trajectories*

The interspike voltage trajectory in normal motoneurones resembles at low current intensities the ahp itself, i.e. is dominated by a hyperpolarizing concavity followed by a linear-convex repolarization. This concavity flattens out with increasing currents and is replaced by a convexity. Thus, at high current intensities, the trajectory describes a convex-linear approach to threshold. It was described in axotomized neurones that the trajectory for all current intensities and for all interspike intervals resembled that in normal motoneurones when high current strength was used, i.e. the trajectory had a convex-linear shape (Heyer & Llinás, 1977). This trajectory behaviour was also occasionally observed in the present study (Fig. 5*A*). The first interval trajectory, starting from the peak of the undershoot, displays already a convex-linear shape at the lowest current strength for rhythmic firing. Increasing the current strength, i.e. changing the slope of the *f–I* curve, gives no obvious change in the trajectory shape. In Fig. 7 are shown the first interval *f–I* curve (*A*) and corresponding trajectories (*B*) for a more typical axotomized neurone. It can be observed that, at the lowest currents, the first interval trajectory shows a clear hyperpolarizing concavity as in normal motoneurones. The trajectory as-

sumes the convex-linear shape only at higher current intensities. This change in trajectory shape could occur at currents close to those giving an upward deviation of the *f–I* curve. In other cells it occurred at appreciably lower current intensities. The same trajectory modifications (from concave to convex shape) occurred invariably for the steady state firing, as illustrated from three representative axotomized motoneurones in Fig. 8*B*, *C*, *D*. In these neurones the steady state *f–I* relations

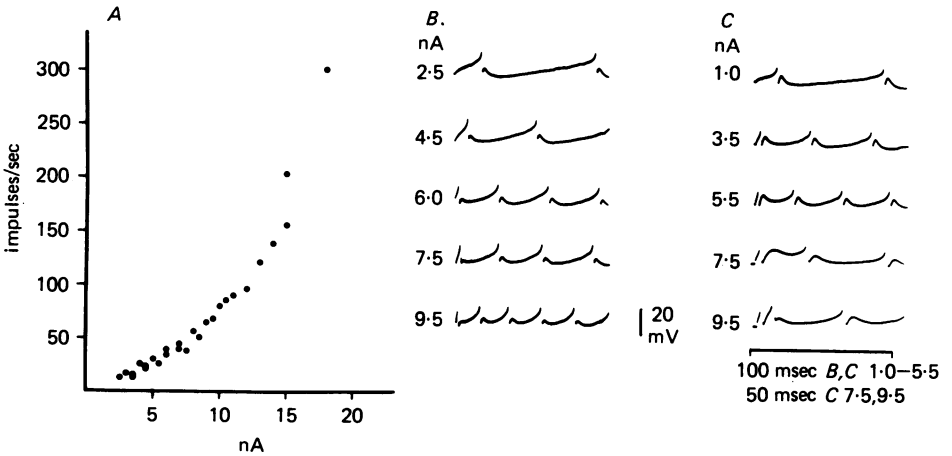


Fig. 7. First interval frequency–current relation in an axotomized motoneurone (after ventral root section). *A*, the reciprocal of the first interval is plotted against the amount of injected current. Each point in the graph represents the average of three trials. *B*, sample records of the first interval trajectories. *C*, another axotomized motoneurone (after ventral root section). For details, see text.

were linear in *C* and *D*, and deviated somewhat upwards (from 2·6 to 3·6 impulses $sec^{-1}$ $nA^{-1}$) for the neurone in *B*. This upward deviation occurred at 25 nA, i.e. well after the trajectory transition to a convex shape. It can also be observed that the trajectory modifications in the axotomized neurones are basically similar to those in the normal motoneurone in *A*. The steady-state *f–I* relation showed an upward deviation in this cell (1·8–2·5 impulses $sec^{-1}$ $nA^{-1}$) at 23 nA. This is well before the trajectory changes to convexity.

All the axotomized neurones in the present study were not tested for the presence of spike-like responses to afferent stimulation as has been done by Heyer & Llinás (1977). There was, however, no obvious difference in firing behaviour between cells where the presence of these partial responses was ascertained and those where it was not. This is illustrated from one cell in Fig. 9. It shows spike-like responses superimposed upon the e.p.s.p.s (*B*), the *f–I* curve deviating upwards for the first interspike interval and the trajectories being concave at low current strength. The slopes of these relations were also within the normal limits for axotomized neurones. In the thirteen cells showing partial responses to afferent stimulation (nineteen cells tested), either of the dome-like or spike-like variety (see Eccles *et al.* 1958), the average steady-state *f–I* slope was 2·7 impulses $sec^{-1}$ $nA^{-1}$, i.e. identical to that of the whole population (see above). Similarly, in the six neurones showing clear spike-like

responses, represented in Fig. 9, the average steady-state slope was even lower, 2·4 impulses $sec^{-1}$ $nA^{-1}$ (ranging from 1·9 to 3·3).

It was shown previously (e.g. Kuno & Llinás, 1970) that the rheobasic current is less following axotomy. Average rheobasic current was $3·9 \pm 1·8$ (S.D.) nA ($n = 23$) for the axotomized neurones. This was significantly lower ($P < 0·02$) than that for

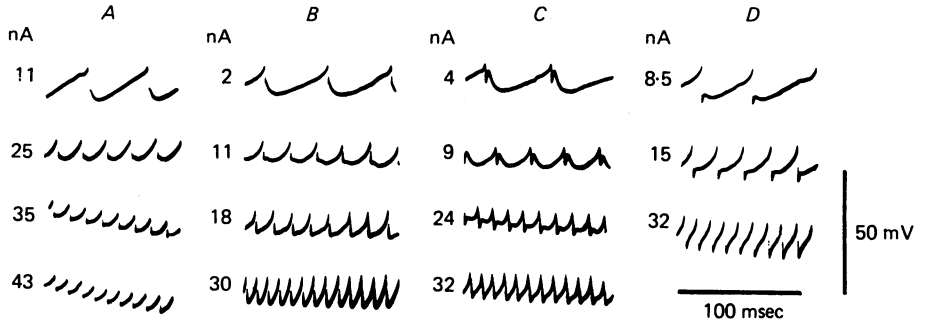


Fig. 8. Steady-state interspike voltage trajectories. *A*, normal motoneurone. *B–D*, three different axotomized motoneurones. Note the general similarity in the trajectory changes between the normal motoneurone (*A*) and the axotomized ones (*B–D*). Changes in the DC level (for example, *A* 43 nA) are related to changes in the electrode resistance. For further details, see text.

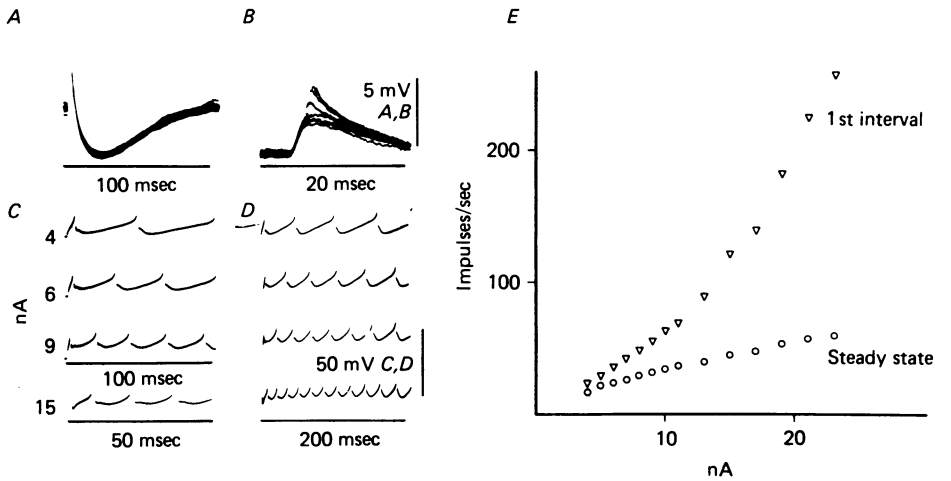


Fig. 9. Frequency–current relation in an axotomized neurone showing partial responses. *A*, afterhyperpolarization following an antidromic spike. *B*, e.p.s.p. evoked by stimulation of the muscle nerve at 1·5 × Th. *C–D*, sample records of the interspike voltage trajectories. *E*, reciprocals of the first interspike interval (open triangles) and the frequency at 0·2 sec (open circles) are plotted against the amount of injected current. The steady-state *f–I* slope is 2·2 impulses $sec^{-1}$ $nA^{-1}$.

normal motoneurones ($8·9 \pm 5·1$ (S.D.) nA, $n = 14$). The 'critical firing level' (rheobasic current × input resistance) was also lower following axotomy, the average being $8·3 \pm 3·7$ (S.D.) mV in axotomized neurones and $10·5 \pm 4·4$ (S.D.) mV in the normal ones. This difference was, however, not significant ($P > 0·05$).

*VI. Direct comparison between real and computed f–I relations*

It was demonstrated in the preceding section that axotomized neurones differ from normal ones in their firing behaviour, in particular by showing a steeper *f–I* slope. As shown in section III there is also less current generated during the ahp following a single spike when comparing axotomized neurones to normal ones. It thus seems reasonable to relate the increase in *f–I* slope to the decrease in ahp current.

This assumption was quantitatively tested for each neurone by comparing the slope of the lower segment of the first interval curve with the *f–I* curve calculated from the ahp current following a single spike. The theoretical *f–I* curves were calculated as follows: the ahp conductance was calculated for each neurone (section III), assuming for all neurones an ahp reversal level 20 mV below resting level. This calculated conductance time course was subsequently approximated by a single exponential line, and its time constant and maximum value were determined. The ahp current at threshold level was then given by this exponential conductance multiplied with the driving force (20 mV plus the difference between resting level and the threshold voltage in the actual cell). The *f–I* curve is then easily derived by calculating the *t* value (and thus *f* value) for any current value (see Kernell, 1968). This derivation of the *f–I* curve neglects the cell capacitance. This omission is of minor importance since the curves were only calculated for frequencies lower than 60–70 impulses/sec.

Fig. 6*B*, *C* shows the experimental and calculated *f–I* slopes for the first interspike interval for normal and axotomized neurones. In Fig. 6*C* are plotted (for each neurone) the experimental and calculated values for normal (filled circles) and axotomized (open circles) neurones. It can be observed that there is a good general agreement between the experimental and calculated *f–I* slopes. Moreover, the shift in the experimental values following axotomy (mean value from 4·2 to 7·2 impulses $sec^{-1}$ $nA^{-1}$) is well matched by the increase in the calculated values (mean value from 4·6 to 8·9 impulses $sec^{-1}$ $nA^{-1}$). Thus changes in *f–I* slope following axotomy can be understood by the decrease in ahp conductance.

## DISCUSSION

In the present study the modifications in firing behaviour were not as extensive as has been reported previously following axotomy (Heyer & Llinás, 1977). The *f–I* relations did not consist of a single linear segment but were usually 'piecewise linear', i.e. deviated upwards at higher frequencies. The interspike voltage trajectories were in general not convex at all current strengths but were, as in normal motoneurones, dominated by a concavity at low current strengths. This similarity to the firing behaviour of normal motoneurones suggests that the firing following axotomy is also regulated by the ahp. This suggestion is supported by the good agreement that was found between the modifications in firing behaviour following axotomy and those expected on the basis of changes in the ahp properties. One would expect that a decrease in ahp conductance following axotomy should lead to an increase in the slopes of the *f–I* relations. Such an increase in slope was indeed found and there was

good quantitative agreement between the decrease of the ahp conductance after a single spike and the increase in the slope of the first interspike interval. The more exponential decay of the ahp conductance following axotomy should also result in a smaller upward deviation of the first interval *f–I* curves and a less frequent crossing of the second and third interval curves (Baldissera & Gustafsson, 1974; Gustafsson, 1974). This was again found experimentally. The decreased incidence in upward deviations of the steady-state *f–I* curves may also be related to changes in other ahp properties such as a more linear summation of successive ahps (Gustafsson, Lindström & Zangger, 1978). This possibility was, however, not tested in the present experiments.

The occasional occurrence of mainly convex interspike voltage trajectories for the first interval (in some of the axotomized motoneurones in the present study) does not imply that the ahp is not controlling the firing in those cells. As earlier discussed (Gustafsson, 1974) and as is obvious from the present results there appears to be no unique relation between the trajectory shape, *f–I* curve shape and underlying mechanism for firing control. Thus, the trajectory shape given by the ahp conductance will depend upon the potentials just succeeding the spike such as the undershoot and the delayed depolarization, on the presence of a plateau in the conductance decay and on the size of the ahp conductance. Different types of trajectories including those being convex at all current strengths can then be obtained (e.g. see fig. 3, Gustafsson, 1974). Changes in the ahp properties following axotomy such as a decrease in ahp conductance, a more exponential decay of the ahp conductance and a large hyperpolarizing undershoot would certainly favour the appearance of convex instead of concave trajectories. This is exemplified by the difference in trajectory shape between motoneurones and spinocerebellar tract cells (Gustafsson, 1974; Gustafsson *et al.* 1978). Thus, in conclusion the present results show that the firing in axotomized neurones is also primarily controlled by the ahp properties.

The present results and conclusion are at variance with those of Heyer & Llinás (1977). Their study on axotomized neurones originated from their working hypothesis that the upward deviation of the *f–I* curves in normal motoneurones is caused by the initiation of dendritic spikes rather than by the ahp properties. These dendritic spikes should then be responsible for the steep *f–I* relation after the upward deviation. Axotomized motoneurones with lower threshold for dendritic spikes should then show a firing with the same characteristics as normal motoneurones after the upward deviation, i.e. a single steep *f–I* relation for all intervals and convex interspike interval trajectories for all intervals and at all current strengths. These predictions were borne out in their study, and they concluded that dendritic spikes were of importance for the initiation of firing with steep *f–I* relations. As discussed above, the present results did not agree with those predictions. Axotomized motoneurones with a high dendritic excitability as evidenced by the presence of spike-like responses on the synaptic potentials showed normal non-linear *f–I* curves with slopes not much steeper than in normal motoneurones and with concave trajectories at low current strengths.

There seems to be no obvious reason for these discrepancies between our results and those of Heyer & Llinás (1977). They might be related to the different criteria used for the identification of axotomized neurones. Heyer & Llinás only used cells

which showed spike-like responses to afferent stimulation. In the present study all cells which could be antidromically activated from the cut ventral roots or nerves were used and not all were tested for the presence of spike-like responses. Although axotomized neurones often show these responses when tested (Kuno & Llinás, 1970) and although there was no apparent difference in the present study between cells showing partial responses and the other cells, this sampling difference might have been of consequence.

It is unlikely that the differences are related to the circumstance that Heyer & Llinás sampled cells with a higher dendritic excitability. First, cells with a proven high dendritic excitability showed even lower than average *f–I* slopes (section III). Further, there was no increased tendency in the axotomized motoneurones in the present study to show upward deviations of the *f–I* curves but rather the reverse. One would not expect this result if these motoneurones had an 'intermediate' rise in dendritic excitability. It is, however, relevant that Heyer & Llinás reported a decreased or almost abolished ahp in their axotomized cells. Such a large reduction in ahp could explain the steeper *f–I* slopes and, as discussed above, the mainly convex trajectories in these cells. Approximately linear *f–I* relations for the first intervals can also be given by models based on the ahp properties (Gustafsson, 1974). It seems therefore reasonable to suggest that the differences in results is related to the sampling of cells with different ahp amplitudes.

The axotomized motoneurones also differed with respect to normal motoneurones in their passive electrical properties. There was a large increase in the input resistance (see, however, Kuno & Llinás, 1970) and a small but significant increase in the membrane time constant. This change in input resistance could either be related to an increase in the specific membrane resistance or to a decrease in cell size. The finding that the electrotonic length as well as the membrane time constant were rather unaffected by axotomy does not correlate with an increase in the membrane resistance but is compatible with a proportional shrinkage of the cells. Retraction of the dendritic tree has also been observed in motoneurones following axotomy (Sumner & Watson, 1971).

There was no change in the ahp peak amplitude following axotomy. This result is in contrast to that of Heyer & Llinás (1977) who found the ahp to be decreased or almost abolished following axotomy (see above). Due to a higher input resistance in axotomized cells, a constant ahp peak amplitude should imply a decrease in the driving force or in the underlying conductance. Measurements of the ahp conductance using current pulses showed that it was rather related to a decrease in the ahp conductance. Axotomized motoneurones generally had a more prominent delayed depolarization than normal motoneurones and this could occasionally facilitate the firing at higher frequencies. This increase could be interpreted as a sign of an increased propagation of the action potential into the dendrites (see Heyer & Llinás, 1977). Alternatively, it could be related to the decrease in ahp conductance, the same current giving a larger potential drop over the increased post-spike resistance.

Huizar, Kuno & Miyata (1975) have earlier suggested that motoneurones 'de-differentiated' following axotomy. This suggestion was based on the finding that the ahp duration in axotomized triceps surae motoneurones returned towards values found in neonatal kittens, i.e. decreased in soleus motoneurones and increased in

mg motoneurones. The present results are in keeping with this idea. Following axotomy, there were no motoneurones with 'fast' characteristics such as short ahp duration and low input resistance. The ahp duration in soleus motoneurones was also decreased. Moreover, the distributions of several parameters such as input resistance, ahp duration and ahp conductance were also narrower following axotomy, approaching almost gaussian distributions. These differences in electrical properties between the populations of normal and axotomized motoneurones are not necessarily caused by changes in the individual cells but could be related to a selective survival of certain kinds of motoneurones following axotomy. This possibility is, though not excluded, not very likely since the changes can also be observed within a homogeneous population of neurones such as the soleus motoneurones (Kuno *et al.* 1974).

When compared to other spinal neurones, e.g. dorsal spinocerebellar tract (dsct) cells, characteristic features of motoneurones are a large ahp conductance, a plateau in the conductance decay, low *f–I* slopes, steep upward deviations of the first interval curve and a tendency to give short first interspike intervals followed by long succeeding ones. As discussed earlier (e.g. Gustafsson, 1974) all these features are important for the functional role of motoneurones in the control of muscle contraction. It is interesting to notice that motoneurones partially lose these characteristics following axotomy and become more similar to dsct cells: a smaller ahp conductance, steeper *f–I* slopes, a presence in many motoneurones of an almost exponential decay of the ahp conductance, more linear *f–I* curves and a smaller difference between a short first interval and the succeeding ones. The trajectory changes are also occasionally similar between axotomized motoneurones and dsct cells (compare fig. 5 with fig. 1, Gustafsson *et al.* 1978). Moreover, motoneurones also show a brief IS-SD delay following axotomy (Eccles *et al.* 1958) and, in addition, a brief hyperpolarizing undershoot and a large delayed depolarization are frequently observed. These are all characteristic features of dsct cells. It thus appears that there is a considerable plasticity in several electrical neuronal properties of motoneurones and that the maintenance of these specific properties is dependent on contact with a muscle (see Czéh, Gallego, Kudo & Kuno, 1978).

## REFERENCES


Baldissera, F. & Gustafsson, B. (1974*a*). Afterhyperpolarization conductance time course in lumbar motoneurones of the cat. *Acta physiol. scand.* **91**, 512–527.

Baldissera, F. & Gustafsson, B. (1974*b*). Firing behaviour of a neurone model based on the afterhyperpolarization conductance time course. First interval firing. *Acta physiol. scand.* **91**, 528–544.

Baldissera, F. & Gustafsson, B. (1974*c*). Firing behaviour of a neurone model based on the afterhyperpolarization conductance time course and algebraic summation. Adaptation and steady state firing. *Acta physiol. scand.* **92**, 27–47.

Baldissera, F., Gustafsson, B. & Parmiggiani, F. (1978). Saturating summation of the afterhyperpolarization conductance in spinal motoneurones. A mechanism for secondary range repetitive firing. *Brain Res.* **146**, 69–82.

Burke, R. E. & Bruggencate, G. ten (1971). Electrotonic characteristics of alpha motoneurones of varying size. *J. Physiol.* **212**, 1–20.

Czéh, G., Gallego, R., Kudo, N. & Kuno, M. (1978). Evidence for the maintenance of motoneurone properties by muscle activity. *J. Physiol.* **281**, 239–252.

ECCLES, J. C., LIBET, B. & YOUNG, R. R. (1958). The behaviour of chromatolysed motoneurones studied by intracellular recording. *J. Physiol.* **143**, 11–40.

EIDE, E. (1968). Input amplifier for intracellular potential and conductance measurements. *Acta physiol. scand.* **73**, 1*A*.

GRANIT, R., KERNELL, D. & LAMARRE, Y. (1966). Synaptic stimulation superimposed on motoneurones firing in the 'secondary range' to injected current. *J. Physiol.* **187**, 401–415.

GUSTAFSSON, B. (1974). Afterhyperpolarization and the control of repetitive firing in spinal neurones of the cat. *Acta physiol. scand.* Suppl. **416**.

GUSTAFSSON, B., LINDSTRÖM, S. & ZANGGER, P. (1978). Firing behaviour of dorsal spinocerebellar tract neurones. *J. Physiol.* **275**, 321–343.

HEYER, C. B. & LLINÁS, R. (1977). Control of rhythmic firing in normal and axotomized cat spinal motoneurones. *J. Neurophysiol.* **40**, 480–488.

HUIZAR, P., KUNO, M. & MIYATA, Y. (1975). Differentiation in motoneurones and skeletal muscles in kittens. *J. Physiol.* **252**, 465–479.

KERNELL, D. (1965). High-frequency repetitive firing of cat lumbosacral motoneurones stimulated by long-lasting injected currents. *Acta physiol. scand.* **65**, 74–86.

KERNELL, D. (1966). Input resistance, electrical excitability and size of ventral horn cells in the cat spinal cord. *Science, N.Y.* **152**, 1637–1640.

KERNELL, D. (1968). Repetitive impulse discharge of a simple neurone model compound to that of spinal motoneurones. *Brain Res.* **11**, 865–867.

KERNELL, D. & SJÖHOLM, H. (1973). Repetitive impulse firing: comparisons between neurone models based on 'voltage clamp equations' and spinal motoneurones. *Acta physiol. scand.* **87**, 40–56.

KUNO, M. & LLINÁS, R. (1970). Enhancement of synaptic transmission by dendritic potentials in chromatolysed motoneurones of the cat. *J. Physiol.* **210**, 807–821.

KUNO, M., MIYATA, Y. & MUÑOZ-MARTINEZ (1974). Differential reaction of fast and slow $\alpha$-motoneurones to axotomy. *J. Physiol.* **240**, 725–739.

RALL, W. (1969). Time constants and electrotonic length of membrane cylinders and neurons. *Biophys. J.* **9**, 1483–1508.

SCHWINDT, P. C. & CALVIN, W. H. (1972). Membrane-potential trajectories between spikes underlying motoneuron firing rates. *J. Neurophysiol.* **35**, 311–325.

SUMNER, B. E. H. & WATSON, W. E. (1971). Retraction and expansion of the dendritic tree of motor neurones of adult rats induced in vivo. *Nature, Lond.* **233**, 273–275.